MANSOURA JOURNAL OF Mathematics
Official Journal of Faculty of Science, Mansoura University, Egypt
E-mail: scimag@mans.edu.eg ISSN: 2974-4946

Thermophoresis of an AerosolCylindrical Particle Embedded in a Micropolar Fluid

Mai Ayman [a], M. S. Faltas [b], H. H. Sherief [b]

[a]Department of Mathematics, Faculty of science, Mansoura University, Mansoura, 35516, Egypt

[b]Department of Mathematics and Computer Science, Faculty of Science, Alexandria University, Alexandria, Egypt

Received: 17/ 3 /2021
Accepted: 8/4/2021

Abstract: The thermophoretic translational motion of an aerosol circular cylindrical object embedded in a gaseous microstructure (micropolar) fluid in the presence of a constant known temperature gradient perpendicular to the axis of the object is investigated analytically. The following assumptions are made: the dissipation function of mechanical energy is neglected, Péclet number is low, the flow is under creeping assumption, and the Knudsen number is supposed to be low such that the fluid flow can be treated as a continuum medium. The heat stress slippage is considered in the analysis of motion in addition to the frictional and creeping slips. The thermophoretic migration of the object is found in a closed form. The effect of micropolarity coefficient on the motion of the particle is discussed and compared with the limiting case of classical viscous fluids. It is found that significant effects on the thermophoretic velocity due to microrotation thermal conductivity coefficient and particle's shape.

keywords: Micropolar fluids. Thermophoretic velocity

1.Introduction

When a heated metal rod immersed in a smoke, we observe that the smoke particles being pushed away, and a particle-free zone is seen, Tyndall [1]. Physically this phenomenon is known as thermophoresis. It is a force caused from a temperature difference colonized in the gaseous medium. An object in that temperature difference produces a force directed along a direction in which the temperature decreases. The thermophoretic force has practical importance in deposition applications, e.g., thermophoresis can be very useful in elimination or compiling tiny objects from fluid streams, in air purification and aerosol sampling equipment [2, 3]. Thermophoresis is one of the important techniques employed to discrete various polymer objects in field flow fractionation. In addition, thermophoresis has been used as a flexible method for treating single biological macro-molecules, such as genomic-length DNA, and HIV virus in micro- and nano-channels [4]. Many other applications are cited in [5 - 10]. Most of the work on thermophoresis were restricted to spherical particles under low Péclet and Knudsen numbers assumptions in the case of creeping flow conditions and taking into account temperature jump, heat creep, thermal stress slip, and mechanical slippage at the object surface. Chang and Keh [11] found the thermophoretic mobility of a spherical object in a uniformly prescribed temperature difference and studied the effect of heat stress slippage on the motion of the particle. Li and Keh [12] treated the problem of thermophoresis of a spherical object moving along the central line of a microtube. Previous studies are constrained to Newtonian classical viscous fluids; however few works are found in the literature investigate the class of micropolar fluids. Saad, Faltas [13] investigated three related problems of thermophoresis of a spherical object immersed in a gaseous microstructure medium and found expressions for thermophoretic mobilities and forces in terms of the micropolarity parameter characterizing the micropolar medium and the heat properties of the fluid and object. In addition, Faltas and Ragab [14] found expressions for thermophoretic mobilities and photophoretic forces of a spherical object immersed in a porous medium as functions of the Brinkman number characterizing the permeability of the medium and the thermal properties of the porous medium and particle. The limiting cases of clear fluid and Darcy's flow besides the case of no-slippage are also discussed.

In practice most aerosol particles are non-spherical; therefore, it is important to study the effect of particle shape on thermophoresis, [15-20]. Chang and Keh [21] analyzed the problem of thermophoresis and photophoresis of an aerosol cylindrical particle moves perpendicular to its axis in the slip-flow system. They calculated the thermophoretic velocity of the particle in an unbounded gas possessing a uniform temperature difference ∇T_∞ as

$$\vec{U} = -A\nabla T_\infty, \quad (1.1)$$

where the thermophoretic mobility

$$A = \left[\frac{C_s\left(k + k_1 C_t \lambda a^{-1}\right) + C_h C_m \lambda a^{-1}\left(k - k_1 + k_1 C_t \lambda a^{-1}\right)}{\left(1 + 2C_m \lambda a^{-1}\right)\left(k + k_1 + k_1 C_t \lambda a^{-1}\right)}\right]\frac{\mu}{\rho T_0}. \quad (1.2)$$

In equation (1.2) k ,$\rho, \mu,$ and are the heat conductivity, density, and viscosity, respectively, of the bulk medium; k_1 is the heat conductivity of the object; T_0 is a scale temperature and $C_s, C_t, C_m,$ and C_h denote to dimensionless coefficients of heat creep slippage, temperature jump, mechanical slippage and heat stress slippage, respectively, at the surface of the object. λ is the mean free path of fluid molecule, and a is the radius of the sphere

The well-established Navier- Stokes equations of the Newtonian fluids has a limitation in describing complex fluids such as colloidal, suspensions and emulsion systems. Eringen [22] initiated the theory of micropolar fluids with microstructure, which is a well-founded and significant generalisation of the classical model of Navier- Stokes equations and covering both in theory and applications. Several experiments show, the micropolar model better represents behavior of various real fluids, especially when the characteristic dimension of the flow is small. The motion of a microstructure (micropolar) fluid is described by two essential qualities: the usual velocity which identify the motion of macro- elements and the microrotation angular velocity which describe the rotation of micro-elements. Numerous studies have been found in the literature for the subject of thermal conductivity of micro structured fluids. The subject of the heat conductivity of micropolar fluids were also developed by Eringen [23] and reviewed by Migun and Prokhorenko [24].

In this work, we consider an exact treatment of the thermophoresis of a circular cylindrical particle embedded in a gaseous micropolar infinite medium in the slippage-flow regime under the action of a temperature difference along a line perpendicular to the axis of the object. An explicit formula for the thermophoretic velocity of the cylindrical object given by expression (1.1) rectified with the micropolarity effect is obtained.

2. Governing Model

In the following analysis, the conservation of mass, linear momentum, angular momentum lows and conservation of energy for the steady flow of an incompressible micropolar fluid under the assumptions of low Péclet number and creeping flow conditions, neglecting the body forces, and couples and also thermal sources are given by [22, 23]:

$$\nabla \cdot \vec{q} = 0, \quad (2.1)$$

$$-\nabla p - (\mu + \kappa)\nabla \wedge \nabla \wedge \vec{q} + \kappa \nabla \wedge \vec{\nu} = 0, \quad (2.2)$$

$$(\alpha + \beta + \gamma)\nabla\nabla \cdot \vec{\nu} + \kappa \nabla \wedge \vec{q} - \gamma \nabla \wedge \nabla \wedge \vec{\nu} - 2\kappa\vec{\nu} = 0, \quad (2.3)$$

$$\nabla \cdot k\nabla T + \rho\Phi = 0, \quad (2.4)$$

where $\rho, \vec{q}, \vec{\nu}$ and p are, respectively, the density, local velocity, micro - angular velocity and the dynamic pressure for micropolar medium. μ is a material coefficient and κ is a vortex second material coefficient, α and β are spin material parameter and γ is the shear spin material parameter. Φ denotes to the density dissipation function due to mechanical energy; its description can be found in [25] and k is the classical thermal conduction factor. Here in our analysis of thermophoresis, we neglect the effect of Φ since all its terms are of second order and consider the thermal conductivity factor k, is uniform throughout the medium. Moreover, if the motion of the micropolar fluid elements are slow and the size of the aerosol particle is small, then all inertia terms in the involved fluid equations and energy equations are neglected. In that situation, the transport of thermal energy between the micropolar medium and the cylindrical object is basically through thermal conduction. Therefore, the temperature of fluid medium satisfies Laplace's equation, which is the same equation for classical viscous fluids under the same physical consideration.

The stress dyadic tensor, Π of the micropolar flow is a nonsymmetric dyadic and is given by the following constitutive relation:

$$\Pi = -pI + \tfrac{1}{2}(2\mu+\kappa)\left(\nabla\vec{q}+\nabla^{*}\vec{q}\right) - \kappa\varepsilon\cdot\left(\vec{\nu}-\vec{\omega}\right), \tag{2.5}$$

where star denotes to the transpose of a quantity, $\vec{\omega}=\frac{1}{2}\,curl\,\vec{q}$ denotes to the vorticity of the fluid, I is the unit tensor, and ε is the permutation tensor. The symmetric part of the stress tensor Π in (2.6) is:

$$\Pi^{[S]} = -pI + \left(\mu+\tfrac{1}{2}\kappa\right)\left(\nabla\vec{q}+\nabla^{*}\vec{q}\right), \tag{2.6}$$

The symmetric tensor $\Pi^{[S]}$ coincides with the stress tensor of the Newtonian viscous fluids, where $\mu_v=\mu+\frac{1}{2}\kappa$ refers to the usual viscosity material coefficient of the classical viscous fluid [26]. Generally, the material viscosity factor μ in the field equation (2.2) is not equal to the material viscosity of the classical viscous Stokes fluid, μ_v. They are the same $(\mu_v=\mu)$ only if κ vanishes. In this situation, equation (2.2) reduces to the Newtonian viscous case and reduces equation (2.5) for the stress dyadic into the usual equation of the stress dyadic of viscous fluid [27]. The couple stress dyadic, m and the thermal vector, $\vec{E}$ are given by the expressions:

$$m = -\frac{\alpha_1(\mu+\kappa)^2\beta}{a^4\rho T_0}\varepsilon\cdot\nabla T + \alpha I\cdot\nabla\vec{\nu} + \gamma\nabla\vec{\nu} + \beta\nabla^{*}\vec{\nu}, \tag{2.7}$$

$$\vec{E} = k\left(\alpha_1\rho T_0\nabla\wedge\vec{\nu} - \nabla T\right), \tag{2.8}$$

where T_0 denotes to a typical temperature value, a is a typical length and α_1 is a thermal conductivity factor due to microrotation. Note that, the appropriate quantities multiplied by α_1 in the above relations are to balance the dimensional scale. It is a matter of importance to observe that the couple stress dyadic and the thermal vector relations (2.7) and (2.8) involve the new terms ∇T and $\nabla\wedge\vec{\nu}$ respectively [28]. Each of these terms multiplied by α_1 which shows that a possible production of thermal energy due the rotation of micro-elements.

3. Mechanical and thermal slip regimes

The "frictional slippage" or the "viscous slip" means the possibility that fluid may slip at the surface of a solid boundary. This condition assumes that the relative tangential velocity of a fluid at a solid boundary is proportional with the tangential stress. The constant of proportionality is known as slippage friction; it depends on the physical properties of the fluid and solid boundary. For the micropolar fluids, an appropriate general form of this condition can be written in the form

$$\vec{q}_1 = \frac{2C_m\lambda}{2\mu+\kappa}(I-\vec{n}\vec{n})\cdot(\vec{n}\cdot\Pi), \tag{3.1}$$

Here $\vec{n}$ is the outward unit normal vector at the surface of the immersed object and λ refers to mean free path of a molecule in a fluid element. The non- dimensional quantity, C_m is in a relation with the momentum accommodation parameter at the solid boundary [29]. The laboratory data and analytical investigations show that it depends on the type of the surface and the surrounding fluid and its value in the range of 1.0–1.5 [30, 31]. The fact that the gas or fluid molecules which are in contact with the surface of the immersed object can slip appears in various physical circumstances such as the rarefied gas stream around a colloidal particle [32–33], the aqueous fluid stream in touch with a hydrophobic surface [34–36], the micropolar fluid stream surrounding a rigid object [37], and the viscous fluid stream around the surface of a porous particle [38,39] or a microparticle of molecular size [40], have been settled experimentally.

A second velocity slip, called "creeping slip", appears when the solid and the adjacent fluid affected by a temperature gradient. This velocity slip can be expressed for micropolar as

$$\vec{q}_2 = -\frac{C_s(2\mu+\kappa)}{2\rho T_0 k}(I-\vec{n}\vec{n})\cdot\vec{E}, \tag{3.2}$$

where C_s is called the heat creep factor and its value ranges around 1. The creeping velocity slippage expresses heat creep stream that is produced by the longitudinal temperature difference around the surface of the object. The creeping velocity slip is important and included in many physical applications such as gas flow through vacuum equipment and microchannel [41].

In addition to the above velocity slips there is a third velocity slip named as heat stress slip; its expression for micropolar fluids is

$$\vec{q}_3 = \frac{C_h(2\mu+\kappa)}{2\rho T_0 k}C_m\lambda(I-\vec{n}\vec{n})\cdot(\vec{n}\cdot\nabla\vec{E}). \tag{3.3}$$

Here the coefficient C_h is named as the heat stress slip and its estimated value around 1. It should be noted that the coefficient C_h will be eliminated if the viscous slippage C_m equals zero. This condition was initiated by Sone [42] and reviewed by Bakanov [43] in his analytical investigations of thermophoretic bodies of high thermal conduction. It is obvious from condition (3.3), this velocity slip is proportional to the tangential rate in the normal temperature difference. In fact, the early studies of Maxwell [44] suggested a refinement heat stress term in the slippage-flow equation, but it has been cancelled over time, possibly due to its less importance in total of slippage effects. Some authors tested the usefulness of heat stress versus the studies neglecting this effect [11, 45, 46]. They concluded that the thermophoretic forces applied on the object are in perfect agreement with laboratory data in comparison with the results obtained by Brock [47] and Mackowski [48] in the absence of heatstress slip.

In association with the frictional stress slip, Saad and Faltas [13] proposed an appropriate general condition for the spin slip, $\vec{\nu}_s$ at the surface of the solid object in the form

$$\vec{\nu}_s = \frac{C_n\lambda}{\beta}(I-\vec{n}\vec{n})\cdot(\vec{n}\cdot\mathrm{m}), \tag{3.4}$$

Here, again C_n is a dimensionless frictional spin slippage coefficient. The actual values of C_n are not determined yet experimentally. However, we expect that its value around the values of C_m. In general, C_n is not the same as C_m

4.Mathematical formulation of thermophores problem

Consider a two-dimensional case of a thermophoresis of a long circular cylindrical object. The radius of the cylinder is denoted by a with heat conductivity k_p , The cylinder embedded in an infinite micropolar region. Let $k,\ \alpha_1$ represent the heat conductivities of the micropolar fluid region. The origin of the Cartesian and cylindrical frame of reference (x,y,z) and (r,θ,z), respectively, is located at the center of the cross section of the object with corresponding unit vectors $(\vec{i},\vec{j},\vec{e}_z)$ and $(\vec{e}_r,\vec{e}_\theta,\vec{e}_z)$. The cylindrical particle is moving perpendicular to $z-$axis (the axis of cylinder) with constant velocity $U\vec{i}$ (U is unknown). Allowing for mechanical and heat slips at the surface of the cylinder. The resulting motion is steady. At infinity, we impose a uniform temperature difference, $\nabla T_\infty\left(=-E_\infty\vec{i}\right)$,

in which $E_\infty > 0$ (see Fig.1). Our purpose in this paper is to calculate the thermophoretic mobility of the object including the mechanical slippage term given by (3.1), heat creep term given by (3.2), heat stress slip term given by (3.3), besides to the mechanical spin slippage term.

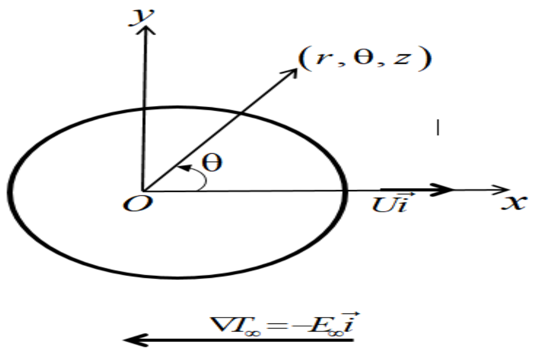

Fig. (1): Coordinate graph of th thermophoresis of cylindrical object

Obviously, the temperature T_∞ far from the object, is as follows,

$$T_\infty(x) = T_0 - E_\infty x, \quad (x = r\cos\theta) \qquad (4.1)$$

Here T_0 is a known constant. The quantity aE_∞ / T_0 is named Epstein coefficient. In practical, this coefficient has a low value [49].

The main aim of this article is to examine the effect of the micropolar medium, on the thermophoretic mobility of the object.

Analysis of stream function*:*

In the case of two dimensional motion of an incompressible micropolar fluid, the velocity and microrotation vectors are of the form

$$\vec{q}(r,\theta) = q_r\vec{e}_r + q_\theta\vec{e}_\theta, \qquad (4.2)$$

$$\vec{\nu}(r,\theta) = \nu\vec{e}_z. \qquad (4.3)$$

From the incompressibility equation (2.2), it is convenient to let the components (q_r, q_θ) of velocity such that

$$q_r = \frac{1}{r}\frac{\partial\psi}{\partial\theta}, \qquad q_\theta = -\frac{\partial\psi}{\partial r}, \qquad (4.4)$$

where ψ is Stokes's stream function. Substitute from (4.2) - (4.4) into the flow equations (2.2) and (2.3), we get

$$\frac{\partial p}{\partial r} = \frac{\mu+\kappa}{r}\frac{\partial\nabla^2\psi}{\partial\theta} + \frac{\kappa}{r}\frac{\partial\nu}{\partial\theta}, \qquad (4.5)$$

$$-\frac{1}{r}\frac{\partial p}{\partial\theta} = (\mu+\kappa)\frac{\partial\nabla^2\psi}{\partial r} + \kappa\frac{\partial\nu}{\partial r}, \qquad (4.6)$$

$$-\kappa\nabla^2\psi - 2\kappa\nu + \gamma\nabla^2\nu = 0, \qquad (4.7)$$

where $\nabla^2 \equiv \frac{\partial^2}{\partial r^2} + \frac{1}{r}\frac{\partial}{\partial r} + \frac{1}{r^2}\frac{\partial^2}{\partial\theta^2}.$

The governing system of equations can be further reduced to the following equations for ψ and ν:

$$\nabla^4\left(\nabla^2 - \ell^2\right)\psi = 0, \qquad (4.8)$$

$$\nu = -\tfrac{1}{2}\left(\nabla^2\psi_1 + 2\tilde{\kappa}\ell^2\psi_2\right), \qquad (4.9)$$

where,

$$\ell^2 = a^2\kappa(2\mu+\kappa)/((\mu+\kappa)\gamma), \quad \tilde{\kappa} = 1 + \mu/\kappa$$

$$\psi = \psi_1 + \psi_2, \quad \ldots\ldots\ldots (4.10)$$

$$\nabla^4\psi_1 = 0, \quad \ldots\ldots\ldots (4.11)$$

$$\left(\nabla^2 - \ell^2\right)\psi_2 = 0. \qquad (4.12)$$

The general solutions of equations (4.11) and (4.12), which are appropriate to the present problem, are given respectively by

$$\psi_1 = \left(a_1 r^{-1} + a_2 r + c_1 r^3 + c_2 r\ln r\right)\sin\theta, \qquad (4.13)$$

$$\psi_2 = \left(b_1 K_1(\ell r) + b_2 I_1(\ell r)\right)\sin\theta, \qquad (4.14)$$

where the functions I_n, K_n are the modified Bessel of the first and second kind of order n. The unknown constants a_1, a_2, c_1, c_2, b_1, and b_2 are to specified using the imposed boundary conditions at the surface of the object. The radial distance in equations (4.13), (4.14) and in all subsequent relations in this article are normalized with respect to the radius *a* of the object and also the parameter, ℓ. Inserting (4.10), (4.13) and (4.14) into (4.4) and (4.9) we obtain the components of velocity and microrotation as

$$q_r = \left(a_1 r^{-2} + a_2 + c_1 r^2 + c_2\ln r + r^{-1}\left(b_1 K_1(\ell r) + b_2 I_1(\ell r)\right)\right)\cos\theta, \qquad (4.15)$$

$$q_\theta = -\left(-a_1 r^{-2} + a_2 + 3c_1 r^2 + c_2(1+\ln r) + b_1 K_1'(\ell r) + b_2 I_1'(\ell r)\right)\sin\theta, \qquad (4.16)$$

$$a\nu = -\left(4c_1 r + \tilde{\kappa}\ell^2\left(b_1 K_1(\ell r) + b_2 I_1(\ell r)\right)\right)\sin\theta, \qquad (4.17)$$

where dashes denote to differentiation. At infinity the components of velocity and microrotation must be bounded that is

$$q_r \to 0, \quad q_\theta \to 0, \quad \nu \to 0 \quad \text{as} \quad r \to \infty. \qquad (4.18)$$

To satisfy condition (4.18), we must set $a_2 = c_1 = c_2 = b_2 = 0$.

5. Heat transfer through fluid and particle

Under the assumptions stated above, the governed equation satisfied by temperature in the fluid medium is

$$\nabla^2 T = 0, \quad a < r < \infty, \qquad (5.1)$$

and the temperature inside the object is given by

$$\nabla^2 T_p = 0, \; 0 \le r \le a \qquad (5.2)$$

Assume the heat vectors of the fluid medium and inside the object has the forms:

$$\vec{E} = E_r \vec{e}_r + E_\theta \vec{e}_\theta, \qquad (5.3)$$

$$\vec{E}_p = E_{pr} \vec{e}_r + E_{p\theta} \vec{e}_\theta, \qquad (5.4)$$

where the expression of $\vec{E}$ is given by (2.8) and

$$\vec{E}_p = -k_p \nabla T_p \quad 0 \le r \le a, \qquad (5.5)$$

with k_p represents the heat conductivity of the object. The heat flux at the surface of the object is continuous; while we assume a temperature jump at the interface between fluid and object proportional to the heat flux. At large distances from the object the temperature of the fluid remains constant

Also, the temperature inside the object is finite everywhere therefore , the boundary conditions are

$$\vec{E} \cdot \vec{e}_r = \vec{E}_p \cdot \vec{e}_r, \qquad \text{on} \quad r = 1 \qquad (5.6)$$

$$T - T_p = -\frac{C_t \lambda}{k} \vec{E} \cdot \vec{e}_r, \qquad \text{on} \quad r = 1 \qquad (5.7)$$

$$T \to T_\infty = T_0 - aE_\infty r \cos\theta, \qquad \text{as} \quad r \to \infty \qquad (5.8)$$

$$T_p \text{ is finite}, \qquad \text{as} \quad r \to 0 \qquad (5.9)$$

Here C_t is the dimensionless jump factor. This factor is a semi-empirical and is of the order unity. The jump factor C_t can be calculated using the expression: $C_t \approx 1.875(2 - f_t)/f_t$ [50, 51], where f_t refers to the heat accommodation coefficient at the the object-fluid interface. The solution of the differential equations (5.1) and (5.2), subject to the associated boundary conditions (5.6) -(5.2) are found to be

$$T = T_0 - aE_\infty \left(1 + \frac{1}{\Delta_0} \left(\delta_0 - \tilde{k} - \frac{\delta_0 \eta \rho T_0}{\kappa E_\infty} \ell^2 b_1 K_1(\ell) \right) \frac{1}{r^2} \right) r \cos\theta, \qquad (5.10)$$

$$T_p = T_0 - \frac{aE_\infty}{\Delta_0} \left(2 - \frac{\eta \rho T_0}{\kappa E_\infty} \ell^2 b_1 K_1(\ell) \right) r \cos\theta, \qquad (5.11)$$

where $\Delta_0 = 1 + \tilde{k}\tilde{C}_t + \tilde{k}$, $\delta_0 = 1 + \tilde{k}\tilde{C}_t$, $\tilde{C}_t = C_t \lambda / a$, $\tilde{k} = k_p / k$ is the heat conductivity ratio and $\eta = \alpha_1 (\mu + \kappa)/a^2$ is the second heat conductivity parameter due the spin of microelement. Note that the constant b_1 that appears in the above expressions of T and T_p, is not yet calculated; it will be specified from the imposed conditions at the surface of the object. If we omit the terms involving the constant b_1 from the above expressions of T and T_p, we obtain the corresponding values reported by Chang and Keh [17].

6. Kinematic and dynamic conditions

To find the remining constants a_1, b_1 of the flow and the unknown velocity U, the kinematic and dynamic (slippage) conditions at the surface of the object must be settled. The kinematic and the slippage conditions (see equations (3.1) - (3.4)) at the solid boundary of the are in the form

$$q_r = U \cos\theta, \qquad (6.1)$$

$$q_\theta = -U \sin\theta + \frac{2C_m \lambda}{2\mu + \kappa} \tau_{r\theta} + \frac{C_s (2\mu + \kappa)}{2} \left(\alpha_1 \frac{\partial \nu}{\partial r} + \frac{1}{\rho T_0 r} \frac{\partial T}{\partial \theta} \right) - \frac{C_m \lambda C_h (2\mu + \kappa)}{2} \left(\alpha^* \frac{\partial^2 \nu}{\partial r^2} + \frac{1}{\rho T_0} \frac{\partial}{\partial r} \left(\frac{1}{r} \frac{\partial T}{\partial \theta} \right) \right), \qquad (6.2)$$

$$\nu = \frac{C_n \lambda}{\beta} m_{rz}. \qquad (6.3)$$

Here in this study, as we are concerned with slip flow of micropolar fluids, it is essential to consider the spin slip condition (6.3). Slippage conditions at the surface of an object for micropolar regions have been utilized for the velocity, but not for spin, by Sherief et al. [52] and Saad [53]. We anticipate that it is practically more really to employ the slippage conditions for velocity and spin since each of them is applied at the same boundary surface and the slip is basically depends on the nature of the solid boundary and the kind of fluid medium [13]. The following expressions are needed

$$\psi = \left(a_1 r^{-1} + b_1 K_1(\ell r)\right)\sin\theta, \quad (6.4)$$

$$q_r = \left(a_1 r^{-2} + b_1 r^{-1} K_1(\ell r)\right)\cos\theta, \quad (6.5)$$

$$q_\theta = \left(a_1 r^{-2} + b_1\left(\ell K_0(\ell r) + r^{-1}K_1(\ell r)\right)\right)\sin\theta, \quad (6.6)$$

$$a\nu = -\tilde{\kappa}\ell^2 b_1 K_1(\ell r)\sin\theta, \quad (6.7)$$

$$a\frac{\partial \nu}{\partial r} = \tilde{\kappa}\ell^2 b_1 r^{-1}\left(\ell r K_0(\ell r) + K_1(\ell r)\right)\sin\theta, \quad (6.8)$$

$$a\frac{\partial^2 \nu}{\partial r^2} = -\tilde{\kappa}\ell^2 b_1 r^{-2}\left(\ell r K_0(\ell r) + \left(2+\ell^2 r^2\right)K_1(\ell r)\right)\sin\theta, \quad (6.9)$$

$$a\tau_{r\theta} = (2\mu+\kappa)\left(-2a_1 r^{-3} - b_1 r^{-2}\left(\ell r K_0(\ell r) + 2K_1(\ell r)\right)\right)\sin\theta, \quad (6.10)$$

$$a^2 m_{rz} = r^{-1}\left(\frac{(\mu+\kappa)\eta\beta}{\rho T_0}\frac{\partial T}{\partial\theta} + \gamma\tilde{\kappa}\ell^2 b_1\left(\ell r K_0(\ell r) + K_1(\ell r)\right)\sin\theta\right), \quad (6.11)$$

$$\frac{1}{r}\frac{\partial T}{\partial\theta} = aE_\infty\left(1 + \frac{1}{\Delta_0}\left(\delta_0 - \tilde{k} - \frac{\delta_0\eta\rho T_0}{\kappa E_\infty}\ell^2 b_1 K_1(\ell)\right)\frac{1}{r^2}\right)\sin\theta, \quad (6.12)$$

$$\frac{\partial}{\partial r}\left(\frac{1}{r}\frac{\partial T}{\partial\theta}\right) = -\frac{2aE_\infty}{\Delta_0}\left(\delta_0 - \tilde{k} - \frac{\delta_0\eta\rho T_0}{\kappa E_\infty}\ell^2 b_1 K_1(\ell)\right)\frac{1}{r^3}\sin\theta. \quad (6.13)$$

Applying conditions (6.1) and (6.3), we obtain the values of the constants a_1 and b_1 as

$$a_1 = U - 2\eta\beta\delta_0\tilde{C}_n K_1(\ell)\Delta_1^{-1}U_0, \quad b_1 = 2\delta_0\eta\beta\tilde{C}_n\Delta_1^{-1}U_0, \quad (6.14)$$

where

$$\left.\begin{aligned}\Delta_1 &= \ell^2\kappa_1\left[\tilde{C}_n\beta\delta_0\eta^2 K_1(\ell) - \Delta_0\left(\gamma\ell\tilde{C}_n K_0(\ell) + \left(\gamma\tilde{C}_n + \beta\right)K_1(\ell)\right)\right],\\ U_0 &= \frac{(2\mu+\kappa)E_\infty}{2\rho T_0},\ \kappa_1 = \frac{2\mu+\kappa}{2\kappa}.\end{aligned}\right\} \quad (6.15)$$

Inserting (6.6), (6.8)-(6.10), (6.12)-(6.14) into the slip condition (6.2), we obtain the normalized thermophoretic velocity, $U_{th} = U/U_0$ of the cylindrical particle as:

$$\left.\begin{aligned}U_{th} = \frac{\delta_0\beta\eta\tilde{C}_n}{\left(1+2\tilde{C}_m\right)\Delta_1}&\Big\{\left(-\left(1+2\tilde{C}_m\right)\ell K_0(\ell)\right) + \kappa_1\ell^2\eta C_s\left(\ell K_0(\ell) + \tilde{k}\Delta_0^{-1}K_1(\ell)\right)\\ &+ \kappa_1\tilde{C}_m C_h\ell^2\eta\left(\ell K_0(\ell) + \left(\ell^2 + 2\tilde{k}\Delta_0^{-1}\right)K_1(\ell)\right)\Big\}\\ &+ \frac{1}{\left(1+2\tilde{C}_m\right)\Delta_0}\left(\delta_0 C_s + \tilde{C}_m C_h\left(\delta_0 - \tilde{k}\right)\right).\end{aligned}\right\} \quad (6.16)$$

The last term in (6.16) represents the normalized thermophoretic velocity of a cylindrical object embedded in an unbounded classical viscous fluid; it recovers the conclusion given by Chang and Keh [21]. It is known that the Stokes equation (4.8) with equation (4.9) for the two-dimensional motion, in the absence of applied temperature gradient is not unique for objects immersed in an infinite micropolar medium. The existence of solution of the present thermophoretic problem is due the effect of thermal slips terms of equation (6.2).

7. Comments

We present here, the comments on the graphs which represent the thermophoretic velocity of the cylindrical object immersed in the considered fluid region under the action of temperature difference given by (6.16). In the process of graphing, we used the following jump and slip non-dimensional numbers: $C_m = 1.14,\ C_t = 2.18,\ C_s = 1.17$ and $C_n = 1.2$; these values are recommended in the literature. We also consider the following values for the viscosity parameters representing spin of micro-elements inside the macroelements, $\beta/\mu a^2 = 0.2,\ \gamma/\mu a^2 = 0.3$ respectively. Also, we consider $\tilde{C}_t = 2\tilde{C}_m,\ \tilde{C}_n = \tilde{C}_m$.

The normalized thermophoretic velocity (mobility) of the cylindrical object is plotted in Figs. **(**2)-**(7)** against different values of the following physical parameters:

i. The heat conductivity ratio $\tilde{k}\left(=k_p/k\right)$

ii. The Knudsen value $Kn\left(=\lambda/a\right)$,

iii. The viscosity κ/μ,

iv. The jump factor $\tilde{C}_t\left(=C_t\lambda/a\right)$, frictional slip $\tilde{C}_m\left(=C_m\lambda/a\right)$, and frictional spin slip $\tilde{C}_n\left(=C_n\lambda/a\right)$ parameters,

v. The heat stress slippage parameter C_h,

vi. The spin heat conductivity factor $\eta\left(=\alpha_1(\mu+\kappa)/a^2\right)$.

The plots in Fig. **(2)** show that non-dimensional thermophoretic mobility, U_{th} decreases monotonically as $\tilde{k}$ increases for a fixed values of λ/a in the slip regime. This clarifies the fact that a relatively large conductivity of the object diminish the local temperature difference and therefore, the effect of heat creep along the surface of the object. For a fixed value of the thermal conductivity $\tilde{k}$, the non-dimensional thermophoretic mobility decrease with an increase of the heat conductivity η due to spin. The plots show also that when the thermal conductivity η is low in the slip flow region: U_{th} increases with a decrease of λ/a in the range of values of $\tilde{k}$ less than 1and U_{th} increases with an increase of λ/a in the range of values of $\tilde{k}$ larger than 1.

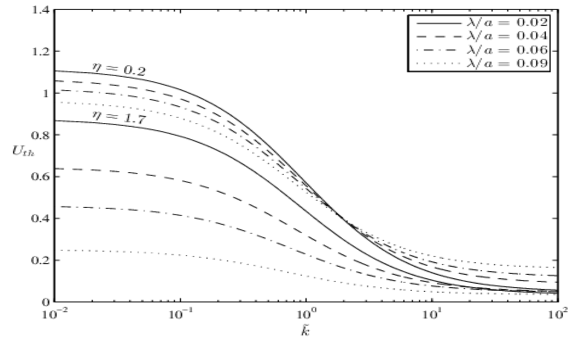

Fig. (2): Plots of the normalized thermophoretic mobility U_{th} against the heat conductivity ratio $\tilde{k}$ for various values of λ/a and η with $C_h=0, \kappa/\mu=4$.

However, for large values of η, the mobility U_{th} increase with the decrease of λ/a for a given value of $\tilde{k}$ in its entire range.

The plots in Fig. **(3)** show the non-dimensional thermophoretic mobility U_{th} against the viscosity ratio κ/μ. It shows, the normalized thermophoretic velocity decreasing with the increase of the micropolarity parameter. This means maximum values of U_{th} reached for the Newtonian viscous media. The dashed plots (with $C_h=0$) indicate the case no-heat stress slip. It can be noted that the implement of heat stress slippage can be powerful when the value of the Knudsen value is not very small or when the size of the object is not very large The effect of C_h is very weak for very small values of λ/a.

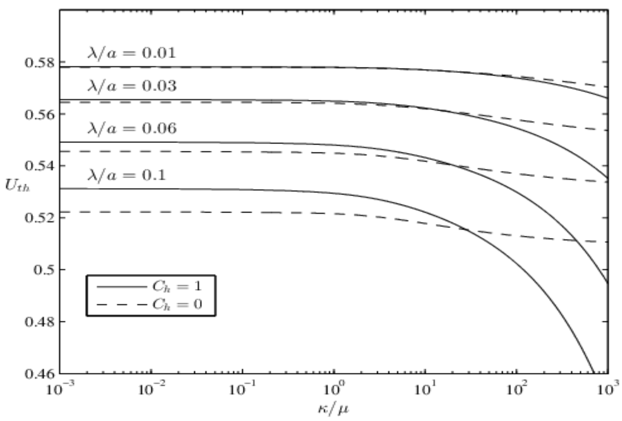

Fig. (3): Plots of the mobility U_{th} against κ/μ for various values of λ/a and C_h with η=0.2, $\tilde{k}=1$.

graphs of the non-dimensional thermophoretic mobility U_{th} against the Knudsen number λ/a are exhibited in Fig. **(4)**. It indicates that in the slippage range, the thermophoretic mobility U_{th} decreases as λ/a increases for $\tilde{k}<1$ and U_{th} increases with the increase of λ/a for $\tilde{k}>1$. The effect of heat conductivity η due spin is low when the value of λ/a approaches zero. Note that, in the plots including the heat conductivity ratio $\tilde{k}$, we considered values of $\tilde{k}$ less than one for comparison.

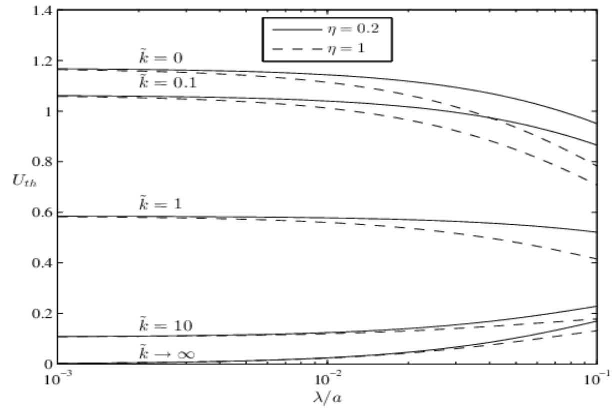

Fig. (4): graphs of the mobility U_{th} against the λ/a for various values of $\tilde{k}$ and η with C_h=0, $\kappa/\mu = 2$.

Again, Fig. **(5)** show plots of the normalized thermophoretic mobility U_{th} against λ/a. It indicates that for various values of the mechanical slippage $\tilde{C}_m$, the mobility U_{th} increases with the increase of Knudsen number in the slippage range. Again, the effect of heat slippage is low for very small values of Knudsen number.

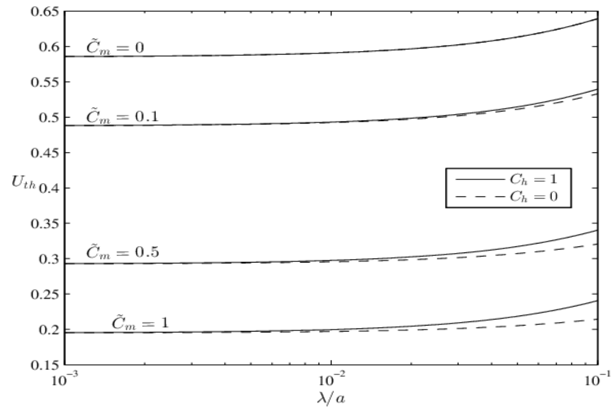

Fig. (5): graphs of the mobility U_{th} against λ/a for various values of $\tilde{C}_m$ and C_h with η=0.2, $\kappa/\mu = 2$, $\tilde{k} = 1$.

Fig. **(6)** show the plots of mobility U_{th} against the ratio $\tilde{k}$. It indicates that, U_{th} has the largest values for the case of continuous temperature at the interface of solid/fluid.

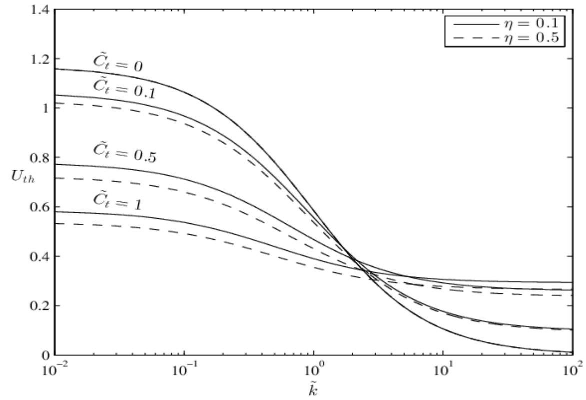

Fig. (6): graphs of the mobility U_{th} against the ratio $\tilde{k}$ for various values $\tilde{C}_t$ and η with $\tilde{C}_t = 2\tilde{C}_m, \tilde{C}_n = \tilde{C}_m, C_h$=0, $\kappa/\mu = 5$.

Fig. **(7)** show the graphs of the mobility U_{th} against κ/μ. It indicates that the effect of micropolarity is weak for values of $\kappa/\mu < 1$.

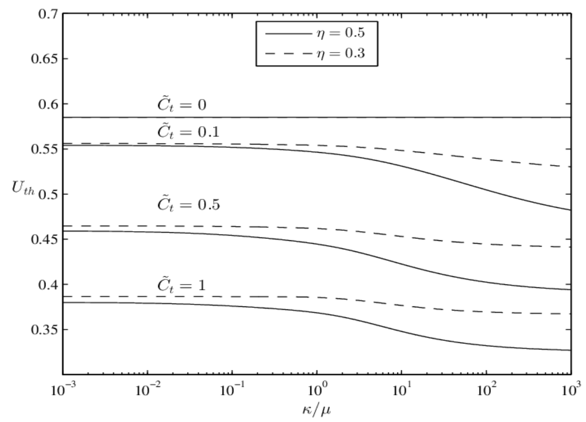

Fig. (7): graphs of the mobility U_{th} against κ/μ for various values of the temperature jump parameter $\tilde{C}_t$ and η with $\tilde{C}_t = 2\tilde{C}_m, \tilde{C}_n = \tilde{C}_m, C_h$=0, $\tilde{k} = 1$.

Figs. **(8), (9)** and Tables **(1)** and **(2)** show comparisons between thermophoretic velocities of cylindrical particles (present study) and spherical particles (Saad and Faltas [59]). The plots and the values of U_{th} displayed in Tables illustrates that under the same set of thermal and micropolarity parameters, the thermophoretic velocity of spherical particles has larger values than that of the corresponding thermochromic velocity for cylindrical particles.

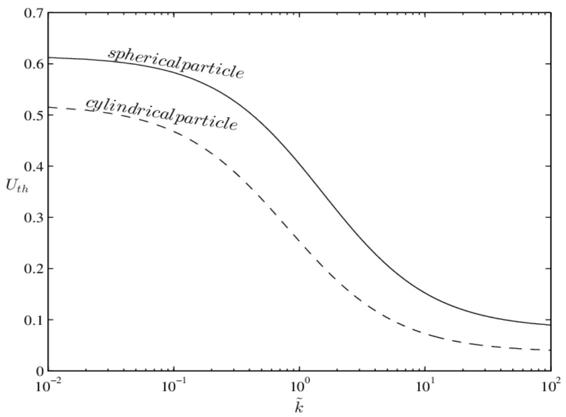

Fig. (8): Comparison of the mobility U_{th} of cylindrical and spherical objects against the ratio $\tilde{k}$ with $\lambda/a = 0.04$, η=1.9, C_h=0, $\kappa/\mu = 4$.

Table (1): Comparison of U_{th} between cylindrical and spherical particles, $\lambda/a = 0.04, \eta$=1.9, C_h=0, $\kappa/\mu = 4$

$\tilde{k}$	U_{th} **(spherical particle)**	U_{th} **(cylindrical particle)**
1	0.4041	0.2533
5	0.2064	0.1041
10	0.1524	0.0730
50	0.0976	0.0444
100	0.0898	0.0406

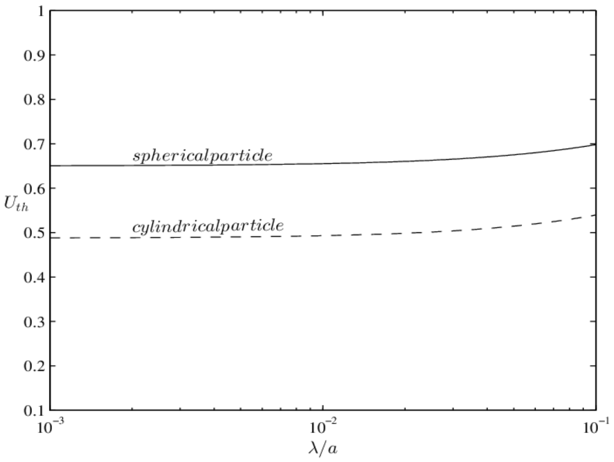

Fig. (9): Comparison of the mobility U_{th} of cylindrical and spherical objects against the ratio λ/a with $\tilde{C}_m$=0.1, C_h=1, η=0.2, $\kappa/\mu = 2$, $\tilde{k} = 1$.

Table (2): Comparison of U_{th} between cylindrical and spherical particles $\tilde{C}_m$=0.1, C_h=1, η=0.2, $\kappa/\mu = 2$, $\tilde{k} = 1$

λ/a	U_{th} **(spherical particle)**	U_{th} **(cylindrical particle)**
0.02	0.6603	0.4986
0.04	0.6703	0.5093
0.06	0.6798	0.5197
0.08	0.6890	0.5298
0.1	0.6978	0.5395

8. Conclusion

In this article, an expression for the thermophoretic velocity of a cylindrical object immersed in an infinite micropolar fluid region is found. The Knudsen is assumed to be very small so that the flow is in the continuum flow regime. The term of heat stress slippage is considered in our investigation and it is found that in general has a significant effect on the thermophoretic mobility of the object. A new thermal coefficient arises from the spin of the microelements characterizing the micropolar gaseous medium. Again, it found that this coefficient has an important significant effect on the mobility of the object.

References

1 J. Tyndall, (1870), On dust and disease, Proc. R. Inst. **6** 1-14.

2 R. Chein, and W. Liao, (2005), Thermophoretic effects on nano-particle deposition in channel flow, Heat. Mass. Transf. **42** 71-79.

3 J. A. Koziel, S. H. Haddadi, W. Koch, and J. Pawliszyn, (2009), Sampling and analysis of nanoparticles with cold fibre SPME device, *J. Sep. Sci*. **32** 1975-1980.

4 C. Zhao, J. Fu, A. Oztekin, X. Cheng, (2014), Measuring the Soret coefficient of nanoparticles in a dilute suspension, *J. Nanopart*. Res. **16** 2625-1-11.

5 N. Montassier, D. Boulaud, and A. Renoux, (1991), Experimental study of thermophoretic particle deposition in laminar tube flow, *J. Aerosol Sci*. **22** 677-687.

6 M.C. Weinberg, (1982), Thermophoretic

efficiency in modified chemical vapor deposition process, *J. Am. Ceram. Soc*. **65** 81-87.

7 Y. Ye, D. Y. H. Pui, B. Y. H. Liu, S. Opiolka, S. Blumhorst, and H. Fissan, (1991), Thermophoretic effect of particle deposition on a free-standing semiconductor wafer in a clean room, *J. Aerosol Sci*. **22** 63-72.

8 M. M. R. Williams, S. K. Loyalka, (1991).Aerosol Science: Theory and Practice, with Special Applications to the Nuclear Industry, Pergamon Press, United Kingdom,

9 A. Messerer, R. Niessner, and U. Poschl, (2003), Thermophoretic deposition of soot aerosol particles under experimental conditions relevant for modern diesel engine exhaust gas systems, *J. Aerosol Sci*. **34** 1009-1021.

10 A. Messerer, R. Niessner, and U. Poschl, (2004), Miniature pipe bundle heat exchanger for thermophoretic deposition of ultrafine soot aerosol particles at high flow velocities, Aerosol Sci. Technol. **38** 456-466.

11 Y. C. Chang, and H. J. Keh, (2012), Effects of thermal stress slip on thermophoresis and Photophoresis, *J. Aerosol Sci*. **50** 1-10.

12 C. Y. Li, H. J. Keh, (2017), Thermophoresis of a spherical particle in a microtube, *J. Aerosol Sci*. **113** 71–84.

13 E. I. Saad, M. S. Faltas, (2019), Theory of thermophoresis of a spherical particle embedded in a micropolar fluid, *J. Mol. Liq***. 282** 527-544.

14 M.S. Faltas and K. E. Ragab, (2019), Thermophoretic and photophoretic velocities and forces of a spherical particle embedded in Brinkman medium, *Eur. Phys. J. Plus*. **134** 475-1-16.

15 M. M. R. Williams, (1986), Thermophoretic Forces Acting on a Spheroid, *J. Phys. D*. **19**1631-1642.

16 H. J. Keh, and C. L. Ou, Thermophoresis of Aerosol Spheroids, Aerosol Sci. Technol. **38** (2004), 675-684.

17 Y. C. Chang, and H. J. Keh , (2009), Thermophoresis of axisymmetric aerosol particles along their axes of revolution, *AIChE. J*. **55** 35-48.

18 Y. C. Chang, and H. J. Keh, (2010), Thermophoretic motion of slightly deformed aerosol spheres, *J. Aerosol Sci.* **41** 180-197.

19 Y. C. Chang, and H. J. Keh, Thermophoresis of axially and fore-and-aft symmetric aerosol particles, Phys. Fluids. **22** (2010), 113305-1-17.

20 H.H. Chen, and H.J. Keh, Thermophoretic motion of a cylindrical particle with chemical reactions, Aerosol Sci. Technol. **48** (2014), 1156-1165.

21 Y. C. Chang, and H. J. Keh, Thermophoresis and Photophoresis of an Aerosol Cylinder with Thermal Stress Slip, Am. *J. Heat. Mass. Transf*. **4** (2017), 85-103.

22 A.C. Eringen, Theory of micropolar fluids, *J. Math. Mech*. **16** (1966), 1-18.

23 A. C. Eringen, Theory of thermomicrofluids, *J. Math. Anal. Appl*. **38** (1972), 480-496

24 N.P. Migun, and P.P. Prokhorenko, Hydrodynamics and Heat Transfer of Gradient Flows of a Microstructural Liquid, Nauka Tekhnika, Russia, (1984).

25 G. Łukaszewicz, Micropolar fluids: Theory and applications, Springer Science and Business Media, New York, (1999).

26 A. K. Piętal, Microchannels flow modelling with the micropolar fluid theory, Bull.Pol. Ac.: Tech. **52** (2004), 209-214.

27 D. Y. Khanukaeva, A. N. Filippov, Isothermal flows of micropolar liquids: Formulation of problems and analytical *solutions, Colloid. J*. **80** (2018), 14-36.

28 Y. Kazakia, T. Ariman, Heat conducting micropolar fluids, Rheol. Acta. **10** (1971), 319-325.

29 E.H. Kennard, Kinetic Theory of Gases, McGraw-Hill, New York, (1938).

30 M. H. Davis, Collisions of small cloud droplets: gas kinetic effects, *J. Atmos. Sci*. **29** (1972), 911-915.

31 L. Talbot, R. K. Cheng, R.W. Schefer, and D. R. Willis, Thermophoresis of particles in heated boundary layer, *J. Fluid. Mech*. **101** (1980), 737-758.

32 D. K. Hutchins, M. H. Harper, and R.L. Felder, (1995), Slip correction measurements for solid spherical particles

by modulated dynamic light scattering, Aerosol. Sci. Technol. **22** 202- 218.
33 F. Sharipov, and D. Kalempa, Velocity slip and temperature jump coefficients for gaseous mixtures. I. Viscous slip coefficient, Phys. Fluids. 15 (2003), 1800-1806.
34 R.S. Myong, J. M. Reese, R.W. Barber, and D. R. Emerson, Velocity slip in microscale cylindrical Couette flow: The Langmuir model, Phys. Fluids. **17** (2005), 087105-1-11.
35 D.C. Tretheway, and C.D. Meinhart, Apparent fluid slip at hydrophobic microchannel walls, Phys. Fluids. **14** (2002), L9-L12.
36 C. H. Choi, U. Ulmanella, J. Kim, C. M. Ho, and C. J. Kim, Effective slip and friction reduction in nanograted superhydrophobic microchannels, Phys. Fluids. 18 (2006), 087105-1-8.
37 G. Willmott, Dynamics of a sphere with inhomogeneous slip boundary conditions in Stokes flow, Phys. Rev. E. **77** (2008), 055302- 1-4.
38 G. S. Beavers, and D. D. Joseph, Boundary conditions at a naturally permeable wall, *J. Fluid. Mech*. **30** (1967), 197-207.
39 P. G. Saffman, On the boundary condition at the surface of a porous medium, Stud. Appl. Math. **50** (1971), 93-101.
40 C. M. Hu, and R. Zwanzig, Rotational friction coefficients for spheroids with the slipping boundary condition, *J. Chem. Phys*. **60** (1974), 4354-4357.
41 T. Kanki, Thermal creep flow around a spherical particle suspended near a plate, *Heat Transfer-Jpn*. Res. **27** (1998), 57–73.
42 Y. Sone, Flow induced by thermal stress in rarefied gas, Phys. Fluids. **15** (1972), 1418-1423.
43 S. P. Bakanov, (2004), The nature of thermophoresis of highly heat-conducting bodies in gases, *J. Appl. Math. Mech*. **68** 25-28.
44 J. C. Maxwell, (1879), On stresses in rarefied gases arising from inequalities of temperature, Philos. Trans. R. Soc. **170** 231-256.
45 C. Y. Soong, W. K. Li, C. H. Liu, and P. Y. Tzeng, (2010), Thermophoresis of a microparticlin gaseous media with effect of thermal stress slip, Aerosol Sci. Technol. **44** 1077-1082.
46 C. Y. Soong, W. K. Li, C. H. Liu, and P. Y. Tzeng, (2010), Effect of thermal stress slip on microparticle photophoresis in gaseous media, Opt. Lett. **35** 625-627.
47 J.R. Brock, (1962), On the theory of thermal forces acting on aerosol particles, *J. Colloid Sci*. **17** 768-780.
48 D.W. Mackowski, (1989), Photophoresis of aerosol particles in the free molecular and
slip-flow regimes, *Int. J. Heat. Mass. Transf*. **32** 843-854.
49 J. B. Young, (2011), Thermophoresis of a spherical particle: reassessment, clarification,
and new analysis, Aerosol Sci. Technol. **45**927-948.
50 L. Waldmann, K.H.Schmitt, (1966).Thermophoresis and di-ffusiophoresis of aerosols, In: C. N. Davies (Ed.), Academic Press, New York,
51 H. J. Keh, and H. J. Tu, (2001), Thermophoresis and photophoresis of cylindrical particles, Colloid. Surface. A. 176 213-223.
52 H. H. Sherief, M. S. Faltas, and E. I. Saad, (2008), Slip at the surface of a sphere translating perpendicular to a plane wall in micropolar fluid, Z. Angew. Math. Phys. **59** 293-312.
53 E. I. Saad, (2008), Motion of a spheroidal particle in a micropolar fluid contained in spherical envelope, *Can. J. Phys*. **86** 1039-1056